Computational Mapping of Brain Networks

Marta Moreno-Ortega[1,2], Daniel C. Javitt[1,3], Alayar Kangarlu[1,3]

1. Department of Psychiatry, Columbia University, New York, NY, USA
2. Centro de Investigacion Biomedica en Red de Salud Mental (CIBRSAM), Spain
3. New York State Psychiatric Institute, New York, NY, USA

Abstract— **Magnetic resonance imaging (MRI) has developed into an indispensible diagnostic tool in medicine. MRI has also demonstrated immense potential for researchers who are making progress in every aspect of this modality expanding its applications into uncharted territories. Computational techniques have made major contributions to MRI enabling detection of minute signals from human brain. Functional MRI (fMRI) offers imaging of the mind as well as the brain in the same session. Complex computational tools are used to visualize brain networks that offer a new powerful tool to study the brain and its disorders. Functional connectivity (fc) maps using resting state fMRI (rsfMRI) is computed by detecting temporal synchronicity of neuronal activation patterns of anatomically separated brain regions. But, a great deal of technological advancement, both in hardware and software, had to be made to make computation of brain networks possible. The critical technologies that made computational modeling of functional brain networks possible were high quality gradients for implementation of distortion free fMRI, faster pulse sequences and radio frequency (RF) coils to capture the fluctuation frequency of neuronal activity, and complex post processing computation of brain networks. rsfMRI is capable of detecting brain function that mediate high cognitive processes in normal brain. We aim to ultimately detect the disruption of this mediation in psychiatric patients. We have already obtained functional connectivity in normal subjects using fMRI data during resting state. We did this as a function of spatial resolution to explore the required computational sources and susceptibility effects on the sensitivity of fMRI to anatomic specialization. We provide a conceptual summary of the role of computational techniques in fMRI data analysis. In exploring this question, ultimately MRI's capability in accessing information at the neuronal level comes to surface. We use latest computational tools for analysis of data from human brain and offer a vision for future developments that could revolutionize the use of computational techniques in making neuropsychiatry a quantitative practice.**

Keywords—magnetic resonance imaging; MRI; fMRI, rsfMRI computational mapping; brain networks

I. Introduction

Understanding how human brain works is a fundamentally important topic that has implications on every aspect of life. Success in finding signatures of normal brain function will have a profound effect on diagnostics and therapeutics of neuropsychiatric disorders [1]. In this regard, the role of specific brain structures in normal brain function is an area of research that has gained much traction after the success of many MRI technologies such as resting state fMRI (rsfMRI) [2]. The brain is organized in networks constituted of hubs or nodes anchored in gray matter structures. Default mode network, DMN, is one such network that is active when a person is in an inwardly reflection state, such as during daydreaming and mind-wandering [3]. DMN is believed to be activated when no other task-oriented network is active [4]. This "default" activation is the basis for the name. DMN, among many overlapping networks, plays the fundamental role of subserving networks that carry out different functions [5]. In-vivo detection of these networks is rather challenging and rsfMRI has offered a tool, for the first time, to delineate the functional connections of these networks noninvasively. Visualization of human brain network organization using neuroimaging data in healthy and psychiatric patients requires elaborate computational resources [6]. This is due to the fact that one needs to acquire whole brain fMRI data with high temporal resolution and spatial resolution. The issue of appropriate spatial resolution is what requires a methodic search for the appropriate "scale" at which to sample synchronous fluctuation of brain structures. FMRI requires acquisition of the entire brain image after one excitation that restricts data acquisition to a time scale of about one (time to repetition) TR. To achieve this task within a TR, i.e. about 2 seconds on most scanners, the imaging technique or pulse sequence called echo planar imaging (EPI) must be used that is only capable of obtaining a low resolution image of about 4 mm in-plane unless more advanced techniques such as parallel imaging (PI) [7] and simultaneous multislice (SMS) imaging are incorporated [2]. Furthermore, the post processing of the rsfMRI data also requires extensive computational resources as the frequency of brain oscillations are in 0.1 to 0.01Hz range requiring acquisition of fMRI data in ten minutes or longer to maximize the statistical power of fitting routines.

II. Background

A. Computation of Brain Networks

Brain networks are made up of sets of brain regions whose activities are aimed at specific tasks. Among the brain networks, default mode network (DMN) is a special network that gears into high activity when the mind is not engaged in specific cognitive or behavioral tasks [8]. When brain engages in focused attention on the external environment DMN activities are supposed to be suppressed to let the network specialized in the task to increase its activity [9, 10]. Increases in cognitive load and task difficulty have been associated with increased activation of the fronto-parietal network (FPN), constituted by regions identified as supporting cognitive control and decision-making processes [11], and increased deactivation of the DMN. To observe DMN suppression, we need to find a neuroimaging technique to detect all brain networks. MRI can reveal these networks through a series of

computations carried out on fMRI images acquired from the brain over a long time. Then, fluctuation frequency of each region is computed and synchronous regions, nodes of the same network, are detected from such computations. Such tool will be valuable in determining the functional role of brain regions in health and disease. To find the diagnostic value of DMN suppression to facilitate task-based cognition we aim to search for the most sensitive fMRI-based technique that offers the DMN suppression deficits in severe mental disorders [3, 12]. Considering that the contrast in fMRI is blood-oxygenation-level dependent (BOLD) in both task-based fMRI and rsfMRI, neural activities are divided between stimulus processing and DMN suppression during task-based stimulus [13]. In this review, the role of computational techniques in accurately visualizing the brain networks is highlighted.

B. Need to Accelerate Image Acquisition

There are very few ways to detect signals from human brain non-invasively. Using fMRI, acquisition of data from brain activity at a 3-5 mm resolution has been the staple of neuroscience research in the last two decades. The physiological process that is detected in fMRI is BOLD that fluctuates by about 1% as a result of orchestrated activity at the nodes of functional networks. Such changes are subtle and subject to choice of many imaging parameters and processing techniques. The minute size of such fluctuations require maximizing the stability of signal-to-noise ratio (SNR) detected from the same voxel over time (tSNR) to reflect the true fluctuation of neuronal activities. It is important to know the best resolution at which the BOLD effect of neuronal activities can be detected. The intuitive response to this question is: a resolution matching the size of the nodes of functional networks. But, from imaging viewpoint, the highest possible resolution has been about 3mm isotropic. Posterior cingulate and superior parietal areas of the DMN show larger percentage of BOLD signal change and consistency within and between healthy subjects than anterior areas of the DMN [14], supporting the evidence on DMN regarded as a heterogeneous network [15]. To investigate this matter, we have embarked on a series of studies of rsfMRI at different resolution to find the best resolution to detect functional networks and its dissociations, i.e. anterior and posterior regions in the brain that might need different resolution requirements. Some studies have shown that acquiring data at higher spatial resolutions results in higher functional and spatial specificity [16]. Fluctuations in echo planar imaging (EPI) signal which constitutes resting state fMRI are due to variations in the signal caused by changes in blood oxygenation in various capilary beds. When fluctuations in BOLD signal stemming from two anatomically desperate regions fluctuate at the same frequency f, ($0.01\text{Hz}<f<0.1$ Hz) these regions are assigned to the same network. Another image acquisition parameter that has computational implication in rsfMRI is the total time required to acquire a whole brain image. As we increase the spatial resolution, the number of in-plane pixels and slices required to cover the whole brain increases prolonging the time required for acquisition of a whole brain volume. Considering that temporal resolution, also called time to repetition or TR, is an important factor in determining the fluctuation frequency of BOLD signal, requirement of high spatial resolution works counter to the need for shorter TR or temporal resolution. Strategies for acquiring fMRI data at a rate fast enough to enable high spatial and temporal resolution are limited to increasing SNR or ability to acquire multiple slices at the same time (SMS). The approach for accelerating data acquisition involves (1) parallel imaging (PI) or ability to acquire multiple simultaneous independent images of the same slice and (2) simultaneous acquisition of multiple slices by each detector, SMS. PI and SMS are both rather challenging and their combination increases the computational requirements of data acquisition and recording by an order of magnitude.

C. Image Acquisition and Processing Computations

The data set used to produce images and maps in this paper was acquired on a GE MR750 Discovery MRI (General Electric, Waukesha, WI) scanner equipped with ESE version 24.0 of GE operating system. An EPI with SMS factors of 6 to 8 were used for acquisition of rsfMRI data in this study. We used a 32 channel RF coil (Nova Medical, Wilmington, MA), which carries out 32 readouts within each readout time, typically 10 msec, and up to 8 simultaneous slices, or SMS factor of 8, which also requires simultaneous reading of their data by our detectors [17]. It is shown that higher resolution fMRI data improves tSNR compared to lower resolution in certain brain regions. However, acquisition time for higher resolution images is longer. This fact is further complicated by the computation power required to achieve higher resolution images for the same time duration as low-resolution images are acquired. To elucidate the computational power required for handling such massive data acquisition, a brief summary of the receive chain architecture is in order. The 3T Discovery MR750 includes 32 independent receive channels. The receiver system is connected to image reconstruction architecture known as the Volume Recon Engine (VRE). The 32-channel receiver system is interfaced with a high-density RF coil with 32 independent channels to accelerate image acquisition through parallel imaging techniques. Given the inhomogeneity of the field of view of each RF Coil element, an onboard software tool called ARC (Autocalibrating Reconstruction of Cartesian data) is used to eliminate misregistration errors and artifacts in real time. Traditionally, these artifacts are removed post-acquisition through the use of a calibration scan. The computational power for reconstruction processing is rather critical for data-intensive studies that up until recently were perceived impractical. As imaging speed increases, electrical noise increases proportionally due to the faster application of gradients and RF readout activity per unit time. One solution to this problem is conversion of electrical signals to optical signal soon after detection. GE MR750 uses an optical RF technology, OpTix, that converts the signal from all 32 channels of data reception to optical signal and wirelessly transmits them through the electromagnetically harsh environment of the scanner room. This maximizes SNR and acquisition speed that provides a platform for neuropsychiatric research aimed at detecting neuronal activity of the human brain. Minimization of electrical noise along the imaging chain, optical receivers, in addition to overall image quality, also achieves the necessary system stability. The volume reconstruction engine (VRE) is a 64-bit computer with the capability of 5400 2D FFTs/second (256 x 256 full FOV) real-

time image generation. For data processing, Human Connectome Project (HCP) pipeline was used on an 8-Core Apple MacPro, 3.5GHz using Intel Xeon E5 with 12MB L3 cache and Turbo Boost up to 3.9GHz Configurable to 3.0GHz 8-core processor with 25MB L3 cache or 2.7GHz 12-core processor with 30MB L3 cache. 16GB of DDR3 ECC memory (four 4GB) of 1866MHz DDR3 ECC memory were on board this machine. The graphics processors were Dual AMD FirePro D500 with 3GB of GDDR5 VRAM each 1526 stream processors, 384-bit-wide memory bus, 240GB/s memory bandwidth, and 2.2 teraflops performance. We generated functional connectivity maps between ventral precuneus/posterior cingulate (PC-VP, BA 23/31, location in the Talairach stereoactic space: 4 -52 29) and every brain voxel. Regions of interest comprising the DMN were defined based on the 7 network cortical parcellation [18].

D. Default Mode Network (DMN)

The DMN includes regions that deactivate during processing of external stimuli, including ventromedial prefrontal cortex/rostral anterior cingulate cortex (vmPFC/rACC), posterior cingulate (PCC), retrosplenial cortex (Rsp), lateral parietal cortex (LPC), lateral temporal cortex (LTC), dorsal medial PFC (dmPFC), and hippocampal formation (HF+) [3, 19]. DMN is also activated by cognitive processes that are internally focused, such as mind wandering [20], self-reference [21], remembering the past and planning the future [22]. It is currently understood that higher cognitive functions are distributed among many distant brain regions and is not localized to a specific area of the brain. Complex mental processes are produced by a synchronized activity of a number of network nodes. Resting state fMRI offers an opportunity to probe the hemodynamics implication of neuronal activity in the form of BOLD fluctuations that enables detection of these networks. Studies that monitor BLOD fluctuation during self-reflectance can detect the brain network that is in control of the brain during these high mental functions with access to all regions of the brain involved in this function. Consistent detection of integration of distributed cortical regions demonstrates that they are involved in cognitive activities of higher mental order that are not region specific. DMN, as such network, offers the knowledge of patterns of neural activity and its potential in the diagnosis of neurological and neuropsychiatric disorders has shone limelight on rsFMRI in an unprecedented way. Evaluation of psychiatric disorders like depression, schizophrenia and autism involving connectivity irregularities between nodes of brain networks is producing more convincing evidence for DMN involvement in these disorders [23-25]. The property of DMN that makes it indispensible in neuroscience is that disengagement from internally focused thought processes relies on interactions between DMN and FPN (FPN is constituted of regions identified as supporting cognitive control and decision-making processes) [11, 26]. In contrast to DMN, other large-scale brain networks such as the dorsal attention network (DAN), are engaed for externally directed cognitive tasks [27]. The FPN correlates with the DAN during externally-focused tasks and with the DMN during resting-state and internally-focused tasks; therefore, facilitating a functional interplay between those two networks [11]. The human brain is organized into large-scale intrinsic connectivity networks (ICNs) whose interrelationships are altered during psychological tasks. Such spectacularly complex structure can now be explored by selectively activating its various networks and evaluating their interactions and their impact on behavior. Considering that human brain is composed of 100 billion neurons forming a complex network with far more synapses and connections, these vast interconnected networks form the machine that produces the cognitive function. Among these networks, DMN, which is engaged for internally cognitive processes, competes with networks involved in external task-directed cognition. Based on the rsfMRI studies, DMN reveals that its activities must have been suppressed during goal-oriented higher cognition tasks, showing anticorrelated activity during cognitively demanding processes. Demonstration of such far-reaching verdict, requires accurate detection of large-scale neural networks distributed over the whole brain. Furthermore, the resting baseline must be detected with high accuracy and precision in order to explore its role in interaction with other networks. rsfMRI stood up to this challenge and empowered science with that capability.

An understanding of task-based deactivation of DMN requires further refinement of fMRI techniques to ensure the role of all network components are properly represented in rsfMRI images. More advanced RF coils, higher SMS capability, and compresses sensing (CS) could help approach the threshold of matching the neuronal subunits dimensions by rsfMRI voxel sizes.

III. DISCUSSION

In this study, we present a summary of computational modeling of brain networks. We also discuss the advantages of high resolution at 3T for functional connectivity measurements in the DMN. High resolutions anatomical images (see Fig. 1) are also used for coregistration of rsfMRI maps. BOLD data were acquired at 3T at different isotropic spatial resolutions (1mm, 1.5 mm and 2 mm). A seed-based temporal correlation approach was used to assess the PV-VP functional connectivity within the DMN. PV-VP is considered a major cortical hub linked to the DMN [28]. As we can see in Figs. 2-4, the entire DMN is connected to the main hub. Although T1W images (Fig. 1) visualize details of cortical structures, EPI does not detect architecture of the default network as accurately as T1W images. As such, the mismatch between anatomical and functional maps are larger at lower resolutions. Comparisons of maps acquired at different resolutions in Fig. 2-4 show that the smaller voxels volumes (1 mm isotropic) resolved more details in the anterior- and posterior-DMN structures closest to corpus collosum. This will guarantee a better match between function and anatomy. This feature is crucial in accurate representation of brain networks.

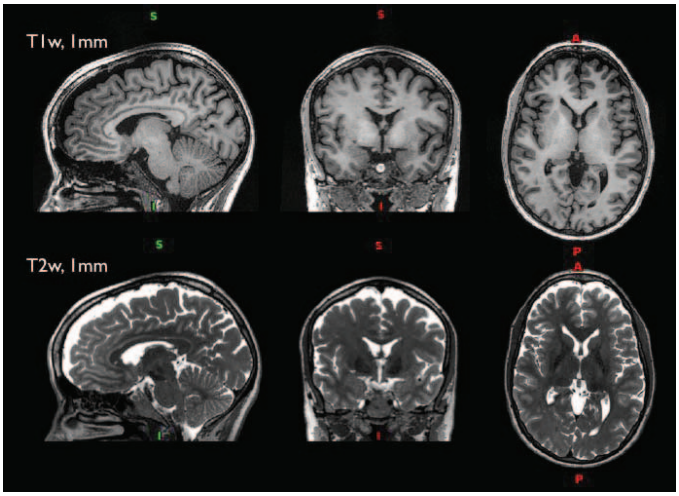

Fig. 1. T1w and T2w images from a representative subject are displayed. High resolution images best visualize small structures in the human brain. (top row, from left) Saggital, coronal, and axial slices of T1W MRI images acquired at 3T show distinct cortical gray matter contrast from underlying white matter structures. Relative values of longitudinal laxation times (T1's) at this field strength work to make white matter to appear "white" and gray matter appear "dark". This is the signature of T1W images in adults in most of life except in newborn infants. (bottom row, from left) Saggital, coronal, and axial slices of T2W MRI images acquired at 3T show gray matter appear lighter than white matter. This is, also, due to relative values of transverse laxation times (T2's) at this field strength work to give T2W images reverse of T1W contrast.

Figures 2-4 show seed-based positive correlation maps across spatial resolutions (1mm, 1.5mm and 2mm) for DMN analyses. A seed in PV-VP cortex results in a connectivity map with the rostral medial prefrontal cortex (rMPFC) as the area of maximal positive correlation, reflecting the midline core set of "hubs" within the default network, defined by their significant correlations with all regions comprising the network. Areas of maximal correlation show PV-VP is strongly connected with a number of medial prefrontal and posterior regions including ventral and dorsal MPFC (or vmPFC and dmPFC, respectively), PCC, retrosplenial cortex (Rsp), lateral temporal cortex (LTC), temporal pole (TempP), posterior inferior parietal lobule (pIPL), parahippocampal cortex (PHC), hippocampal formation (HF+), and temporoparietal junction (TPJ) as areas of maximal positive correlation. Comparing across resolutions although SNR is lower at 1mm and 1.5mm compared to 2mm, more activated voxels are detected in pregenual and subgenual anterior cingulate cortex (pgACC/sgACC) as is shown in Fig. 2. This observation is probably due to lower intravoxel dephasing at higher resolution [29, 30]. The spatial pattern of the DMN is similar across resolutions in other regions. For the DMN at 1mm, the characteristic nodes are observed, with higher degree of functional correspondence with the subject's anatomy (Fig. 4). Improved matching between functional connectivity maps and gray matter anatomy might result from a decrease in intravoxel dephasing affecting BOLD contrast at higher resolutions [31]. The spatial resolution in fMRI is affected by the anatomy of the microcirculation that it can detect. Considering the isotropicity of cortical gray matter structure, carrying out fMRI in smaller cubic voxels will be more sensitive to such microstructure. Furthermore, rsfMRI signal stems from low-frequency BOLD fluctuations that is a response to spontaneous neuronal activities. Noise, however, is dominated by physiological activity of the surrounding tissues supporting the brain within the voxel. So, as it has been modeled [29], high resolution BOLD fMRI may have neuronal information content that is suppressed in low resolution imaging due to averaging across large voxels. This makes certain properties of BOLD signal magnitude a function of its phase content, which varies with resolution. This means that rsfMRI at different resolutions explicitly have access to different information. The use of SMS EPI at 3T magnetic field that is required to achieve subsecond temporal resolution causes a decrease in SNR but fc/anatomy match are improved perhaps due to a closer match between voxels and dimensions of neuronal groups involved in the network. Improvement in hardware, such as stronger and more linear gradients, in future, could lead to a further improvement in BOLD contrast further highlighting this finding.

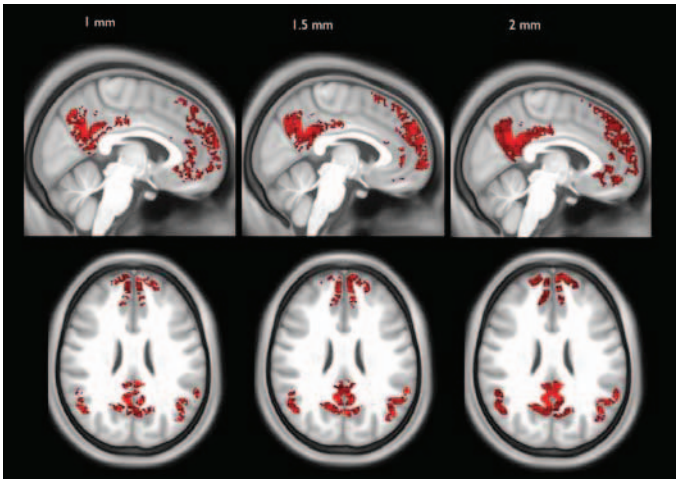

Fig. 2. Average seed-based fcMRI positive correlation maps from PC-VP overlaid onto an average T1w template across spatial resolutions are displayed in sagittal and axial view (Pearson correlation coefficient images). Notice that cortical midline structures (CMS) closest to corpus callosum are better defined at higher resolution (1mm), suggesting the need for a more finely grained spatial scale. CMS refer to brain structures situated near the medial wall of the brain and is mainly comprised of the ventral medial prefrontal cortex, dorsal medial prefrontal cortex, anterior cingulate cortex (the supragenual part in particular) and posterior cingulate cortex.

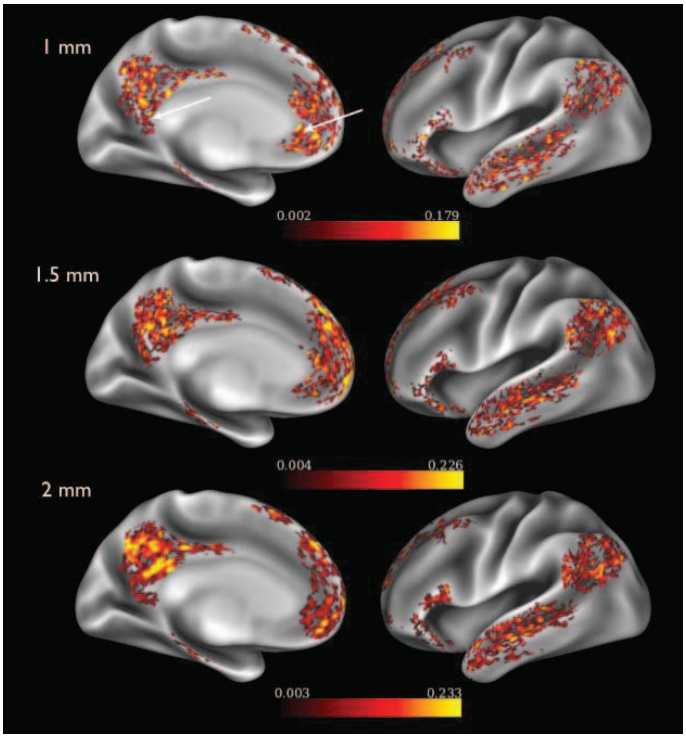

Fig. 3. Average seed-based fcMRI maps from PC-VP projected onto a surface template across spatial resolutions are displayed (Pearson correlation coefficient images). Delineation of the cortical structure representing the architecture of the DMN emerges across all levels of spatial resolution (1mm, 1.5 mm and 2 mm). Notice that anterior-posterior CMS closest to corpus callosum (white arrows) are better detected at higher resolution, i.e. subgneual anterior cingulate cortex (sgACC) and pregenual anterior cingulate cortex (pgACC). Regions detected within the DMN across resolutions are: dorsal medial prefrontal cortex (dMPFC), anterior medial prefrontal cortex (aMPFC), ventral medial prefrontal cortex (vMPFC), posterior inferior parietal lobule (pIPL), temporal parietal junction (TPJ), lateral temporal cortex (LTC), temporal pole (TempP), posterior cingulate cortex (PCC), retrosplenial cortex (Rsp), parahippocampal cortex (PHC) and hippocampal formation (HF+).

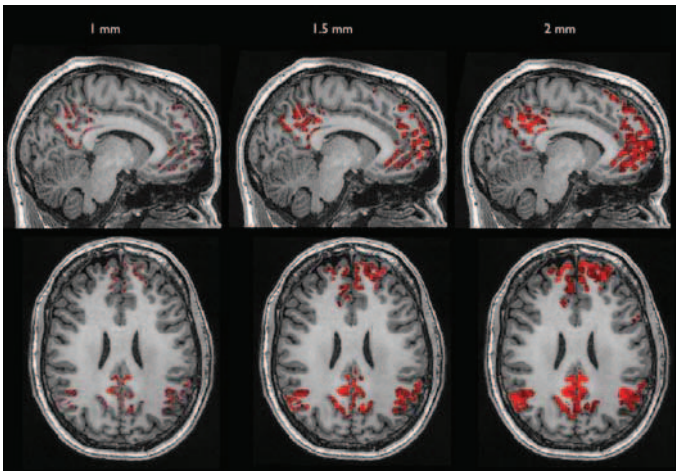

Fig. 4. Seed-based functional-connectivity maps from PC-VP overlaid onto a T1w image for a representative subject across resolutions (1mm, 1.5mm, and 2mm) are displayed. Characteristic nodes are observed across resolutions, with higher degree of functional correspondence with the subject's anatomy at 1-1.5mm resolution. Comparing resolutions, at 1-1.5mm nodes follow more precisely grey matter structures than at 2mm.

IV. CONCLUSION

Computational tools have revolutionized MRI-based study of brain networks. FMRI offered neuroscience a powerful tool to probe the brain at an unprecedented whole brain scale with high resolution. Introduction of techniques such as parallel imaging, simultaneous multislicing, and compressed sensing has greatly accelerated acquisition. In addition to temporal resolution, these techniques have also enhanced spatial resolution in imaging the human brain. Study of brain networks using rsfMRI has offered neuroscience community ability to acquire massive datasets from human brain in a short time. The nature of information embedded in rsfMRI datasets requires complex computational methods to extract the inner secrets of the brain function. Modern MRI scanners capable of visualizing brain networks have onboard reconstruction engine featuring the state-of-art fast memory and local raw data storage to support and maintain simultaneous data acquisition and reconstruction under the massively demanding applications such as SMS EPI. We have learned that in addition to spatial and temporal resolution, the number of image volumes also influences detection of brain networks. This increases the computational demand on fc studies. It is conceivable that the detection power of neuronal activity as revealed by BOLD fluctuations acquired at a spatial resolution comparable to the size of neuronal computation units probe the neuronal networks more accurately. To estimate the computational power required to study the human brain, scientists simulated a network consisting of 1.73 billion nerve cells connected by 10.4 trillion synapses. This simulation took Japan's fastest super computer, K Computer, with 82,944 processors 40 minutes to complete. This was equivalent of 1 second of neuronal network activity of human brain. As such, computational power is critical to acquire, process, and visualize the brain activity. Our present computation tools are approaching brain's computation power from way below and in the process we will be able to shed light on the brain networks acting at a much larger scale than the individual neuronal level. It is so fortunate that with the existing, seemingly meager computational resources neuroimaging has been able to reveal so much!

ACKNOWLEDGMENT

MMO's work has been supported by FCyM (Fundacion Cerebro y Mente), Spain.

REFERENCES

[1] M. Greicius, "Resting-state functional connectivity in neuropsychiatric disorders," *Curr Opin Neurol,* vol. 21, no. 4, pp. 424-30, Aug, 2008.

[2] B. Biswal, F. Z. Yetkin, V. M. Haughton, and J. S. Hyde, "Functional connectivity in the motor cortex of resting human brain using echo-planar MRI," *Magn Reson Med,* vol. 34, no. 4, pp. 537-41, Oct, 1995.

[3] R. L. Buckner, J. R. Andrews-Hanna, and D. L. Schacter, "The brain's default network: anatomy, function, and relevance to disease," *Ann N Y Acad Sci,* vol. 1124, pp. 1-38, Mar, 2008.

[4] J. D. Power, A. L. Cohen, S. M. Nelson, G. S. Wig, K. A. Barnes, J. A. Church, A. C. Vogel, T. O. Laumann, F. M. Miezin, B. L. Schlaggar, and S. E. Petersen, "Functional network organization of the human brain," *Neuron,* vol. 72, no. 4, pp. 665-78, Nov 17, 2011.

[5] Z. Liang, J. King, and N. Zhang, "Anticorrelated resting-state functional connectivity in awake rat brain," *Neuroimage,* vol. 59, no. 2, pp. 1190-9, Jan 16, 2012.

[6] D. C. Van Essen, S. M. Smith, D. M. Barch, T. E. Behrens, E. Yacoub, K. Ugurbil, and W. U.-M. H. Consortium, "The WU-Minn Human Connectome Project: an overview," *Neuroimage,* vol. 80, pp. 62-79, Oct 15, 2013.

[7] D. J. Larkman, J. V. Hajnal, A. H. Herlihy, G. A. Coutts, I. R. Young, and G. Ehnholm, "Use of multicoil arrays for separation of signal from multiple slices simultaneously excited," *J Magn Reson Imaging,* vol. 13, no. 2, pp. 313-7, Feb, 2001.

[8] A. Anticevic, M. W. Cole, J. D. Murray, P. R. Corlett, X. J. Wang, and J. H. Krystal, "The role of default network deactivation in cognition and disease," *Trends Cogn Sci,* vol. 16, no. 12, pp. 584-92, Dec, 2012.

[9] J. S. Mayer, A. Roebroeck, K. Maurer, and D. E. Linden, "Specialization in the default mode: Task-induced brain deactivations dissociate between visual working memory and attention," *Hum Brain Mapp,* vol. 31, no. 1, pp. 126-39, Jan, 2010.

[10] E. Pomarol-Clotet, R. Salvador, S. Sarro, J. Gomar, F. Vila, A. Martinez, A. Guerrero, J. Ortiz-Gil, B. Sans-Sansa, A. Capdevila, J. M. Cebamanos, and P. J. McKenna, "Failure to deactivate in the prefrontal cortex in schizophrenia: dysfunction of the default mode network?," *Psychol Med,* vol. 38, no. 8, pp. 1185-93, Aug, 2008.

[11] J. L. Vincent, I. Kahn, A. Z. Snyder, M. E. Raichle, and R. L. Buckner, "Evidence for a frontoparietal control system revealed by intrinsic functional connectivity," *J Neurophysiol,* vol. 100, no. 6, pp. 3328-42, Dec, 2008.

[12] M. D. Fox, A. Z. Snyder, J. L. Vincent, M. Corbetta, D. C. Van Essen, and M. E. Raichle, "The human brain is intrinsically organized into dynamic, anticorrelated functional networks," *Proc Natl Acad Sci U S A,* vol. 102, no. 27, pp. 9673-8, Jul 5, 2005.

[13] J. R. Binder, "Task-induced deactivation and the "resting" state," *Neuroimage,* vol. 62, no. 2, pp. 1086-91, Aug 15, 2012.

[14] J. S. Damoiseaux, S. A. Rombouts, F. Barkhof, P. Scheltens, C. J. Stam, S. M. Smith, and C. F. Beckmann, "Consistent resting-state networks across healthy subjects," *Proc Natl Acad Sci U S A,* vol. 103, no. 37, pp. 13848-53, Sep 12, 2006.

[15] S. Y. Huang, A. Nummenmaa, T. Witzel, T. Duval, J. Cohen-Adad, L. L. Wald, and J. A. McNab, "The impact of gradient strength on in vivo diffusion MRI estimates of axon diameter," *Neuroimage,* vol. 106, pp. 464-72, Feb 1, 2015.

[16] C. A. Olman, and E. Yacoub, "High-field FMRI for human applications: an overview of spatial resolution and signal specificity," *Open Neuroimag J,* vol. 5, pp. 74-89, 2011.

[17] D. A. Feinberg, S. Moeller, S. M. Smith, E. Auerbach, S. Ramanna, M. Gunther, M. F. Glasser, K. L. Miller, K. Ugurbil, and E. Yacoub, "Multiplexed echo planar imaging for sub-second whole brain FMRI and fast diffusion imaging," *PLoS One,* vol. 5, no. 12, pp. e15710, 2010.

[18] B. T. Yeo, F. M. Krienen, J. Sepulcre, M. R. Sabuncu, D. Lashkari, M. Hollinshead, J. L. Roffman, J. W. Smoller, L. Zollei, J. R. Polimeni, B. Fischl, H. Liu, and R. L. Buckner, "The organization of the human cerebral cortex estimated by intrinsic functional connectivity," *J Neurophysiol,* vol. 106, no. 3, pp. 1125-65, Sep, 2011.

[19] M. E. Raichle, A. M. MacLeod, A. Z. Snyder, W. J. Powers, D. A. Gusnard, and G. L. Shulman, "A default mode of brain function," *Proc Natl Acad Sci U S A,* vol. 98, no. 2, pp. 676-82, Jan 16, 2001.

[20] K. Christoff, A. M. Gordon, J. Smallwood, R. Smith, and J. W. Schooler, "Experience sampling during fMRI reveals default network and executive system contributions to mind wandering," *Proc Natl Acad Sci U S A,* vol. 106, no. 21, pp. 8719-24, May 26, 2009.

[21] A. D'Argembeau, D. Stawarczyk, S. Majerus, F. Collette, M. Van der Linden, and E. Salmon, "Modulation of medial prefrontal and inferior parietal cortices when thinking about past, present, and future selves," *Soc Neurosci,* vol. 5, no. 2, pp. 187-200, 2010.

[22] R. N. Spreng, R. A. Mar, and A. S. Kim, "The common neural basis of autobiographical memory, prospection, navigation, theory of mind, and the default mode: a quantitative meta-analysis," *J Cogn Neurosci,* vol. 21, no. 3, pp. 489-510, Mar, 2009.

[23] T. S. Woodward, K. Leong, N. Sanford, C. M. Tipper, and K. M. Lavigne, "Altered balance of functional brain networks in Schizophrenia," *Psychiatry Res*, Jan 4, 2016.

[24] B. E. Yerys, E. M. Gordon, D. N. Abrams, T. D. Satterthwaite, R. Weinblatt, K. F. Jankowski, J. Strang, L. Kenworthy, W. D. Gaillard, and C. J. Vaidya, "Default mode network segregation and social deficits in autism spectrum disorder: Evidence from non-medicated children," *Neuroimage Clin,* vol. 9, pp. 223-32, 2015.

[25] H. Shi, X. Wang, J. Yi, X. Zhu, X. Zhang, J. Yang, and S. Yao, "Default mode network alterations during implicit emotional faces processing in first-episode, treatment-naive major depression patients," *Front Psychol,* vol. 6, pp. 1198, 2015.

[26] E. R. Stern, K. D. Fitzgerald, R. C. Welsh, J. L. Abelson, and S. F. Taylor, "Resting-state functional connectivity between fronto-parietal and default mode networks in obsessive-compulsive disorder," *PLoS One,* vol. 7, no. 5, pp. e36356, 2012.

[27] J. E. Kragel, and S. M. Polyn, "Functional interactions between large-scale networks during memory search," *Cereb Cortex,* vol. 25, no. 3, pp. 667-79, Mar, 2015.

[28] D. Tomasi, and N. D. Volkow, "Association between functional connectivity hubs and brain networks," *Cereb Cortex,* vol. 21, no. 9, pp. 2003-13, Sep, 2011.

[29] Z. Chen, and V. Calhoun, "A computational multiresolution BOLD fMRI model," *IEEE Trans Biomed Eng,* vol. 58, no. 10, pp. 2995-9, Oct, 2011.

[30] Y. Li, N. Xu, J. M. Fitzpatrick, V. L. Morgan, D. R. Pickens, and B. M. Dawant, "Accounting for signal loss due to dephasing in the correction of distortions in gradient-echo EPI via nonrigid registration," *IEEE Trans Med Imaging,* vol. 26, no. 12, pp. 1698-707, Dec, 2007.

[31] N. Todd, S. Moeller, E. J. Auerbach, E. Yacoub, G. Flandin, and N. Weiskopf, "Evaluation of 2D multiband EPI imaging for high-resolution, whole-brain, task-based fMRI studies at 3T: Sensitivity and slice leakage artifacts," *Neuroimage,* vol. 124, no. Pt A, pp. 32-42, Jan 1, 2016.